A 93-VU-147T cells

D1017587 – 93VU147T

Laboratory Report

Test Requested	Cell Line Authentication
Case Number	10166b
Date Sample Received	25/05/2018
Date Sample Tested	29/05/2018, 30/05/2018
Date Sample Reported	31/05/2018

Sample Name	Sample/Comparison Profile Source	Sample Number	DNA Number
93VU147T	University of Birmingham	S1017587	D1017587
93VU147T - VU-SCC-147	Cellosaurus Database	N/A	N/A

Table of Allelic Data

STR Locus	Genotypes		Match vs. Mis-Match
	93VU147T (Test Sample)	93VU147T - VU-SCC-147 (Database Sample)	
D5	11 | 12	11 | 12	Match
D13	12 | 12	12 | 12	Match
D7	10 | 11	10 | 11	Match
D16	9 | 11	9 | 11	Match
vWA	18 | 18	18 | 18	Match
Amel	X | X	X | X	Match
TPOX	9 | 11	9 | 11	Match
CSF1PO	11 | 12	11 | 12	Match
THO1	7 | 9	7 | 9	Match

Matching Percentage: 100%
Outcome: Related

The outcome percentage is calculated using a formulae which compares the number of alleles present against the number of alleles shared between the two DNA profiles. The outcome is designated one of the following statements based upon the outcome percentage:

Related (>80%)	The Cell Lines are considered to be related.
Inconclusive (56-79%)	Further profiling is required to determine whether the profiles are related.
No Match (55%>)	It is considered that the two cell lines are unrelated.
Misidentified	Cell Lines have been found to match a different donor within the database

Reported By: Ms. Abbey Rutherford (Technical Supervisor)

Authorised By: Mrs. Julie Coaker (Senior Technical Officer)

Date: 31/05/2018

B HeLa cells

D101589 – HELA

Laboratory Report

Test Requested	Cell Line Authentication
Case Number	10166d
Date Sample Received	25/05/2018
Date Sample Tested	29/05/2018, 30/05/2018
Date Sample Reported	31/05/2018

Sample Name	Sample/Comparison Profile Source	Sample Number	DNA Number
HELA	University of Birmingham	S1017589	D1017589
HeLaCervical AdenocarcinomaHuman	ATCC Database	N/A	N/A

Table of Allelic Data

STR Locus	Genotypes		Match vs. Mis-Match
	HELA (Test Sample)	HeLaCervical AdenocarcinomaHuman (Database Sample)	
D5	11 | 12	11 | 12	Match
D13	12 | 13.3	12 | 13.3	Match
D7	8 | 12	8 | 12	Match
D16	9 | 10	9 | 10	Match
vWA	16 | 18	16 | 18	Match
Amel	X | X	X | X	Match
TPOX	8 | 12	8 | 12	Match
CSF1PO	9 | 10	9 | 10	Match
THO1	7 | 7	7 | 7	Match

Matching Percentage: 100%
Outcome: Related

The outcome percentage is calculated using a formulae which compares the number of alleles present against the number of alleles shared between the two DNA profiles. The outcome is designated one of the following statements based upon the outcome percentage:

Related (>80%)	The Cell Lines are considered to be related.
Inconclusive (56-79%)	Further profiling is required to determine whether the profiles are related.
No Match (55%>)	It is considered that the two cell lines are unrelated.
Misidentified	Cell Lines have been found to match a different donor within the database

Reported By: Ms. Abbey Rutherford (Technical Supervisor)

Authorised By: Mrs. Julie Coaker (Senior Technical Officer)

Date: 31/05/2018

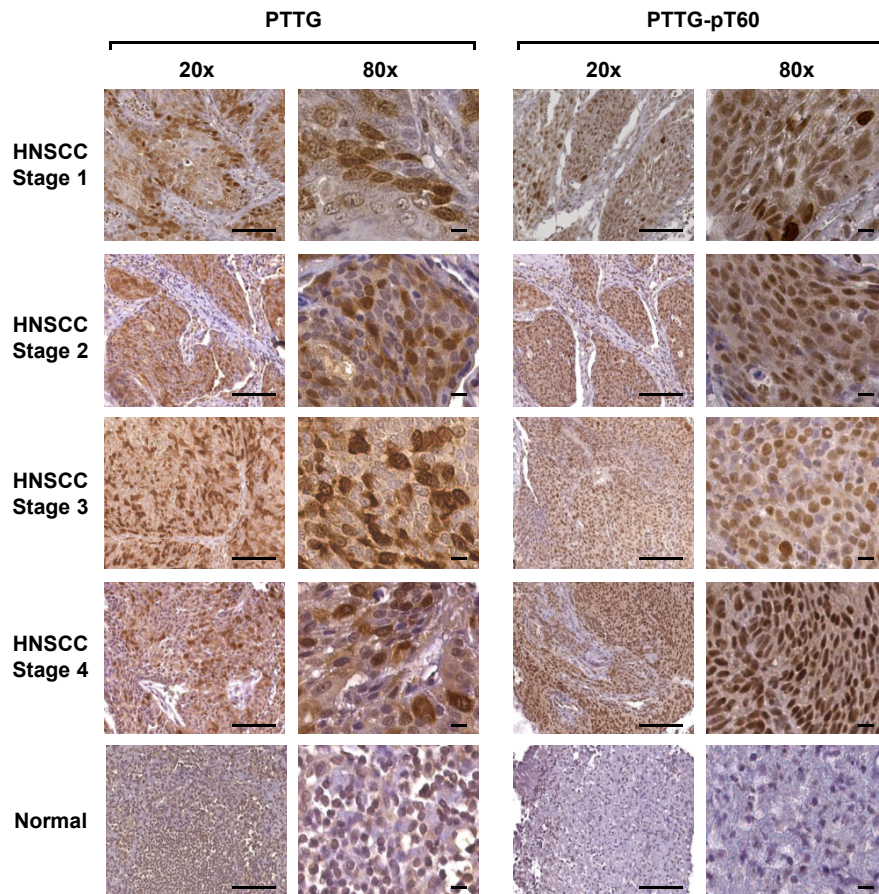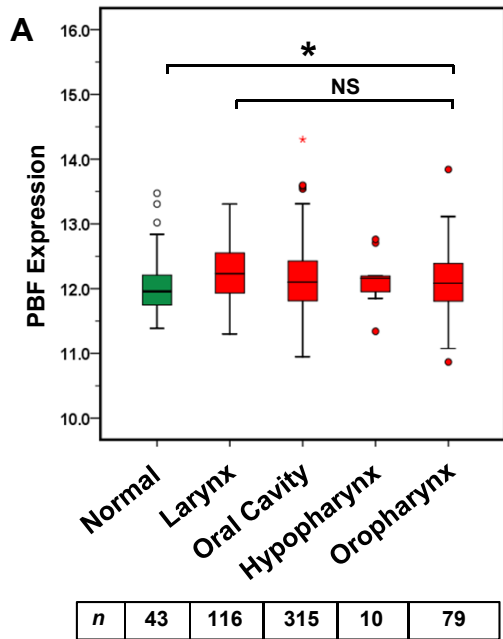**Supplementary Figure S1.** Representative examples of short tandem repeat (STR) profiling. Panels A-B show a representative copy of the electropherogram and Cell Line DNA Typing report obtained following STR analysis by the accredited company NorthGene (Newcastle upon Tyne, UK). The authenticity was assessed by comparing the generated Short Tandem Repeat (STR) profile with the source STR profiles present in the American Type Culture Collection, Cellosaurus and the Deutsche Sammlung von Mikroorganismen und Zellkulturen (DSMZ).
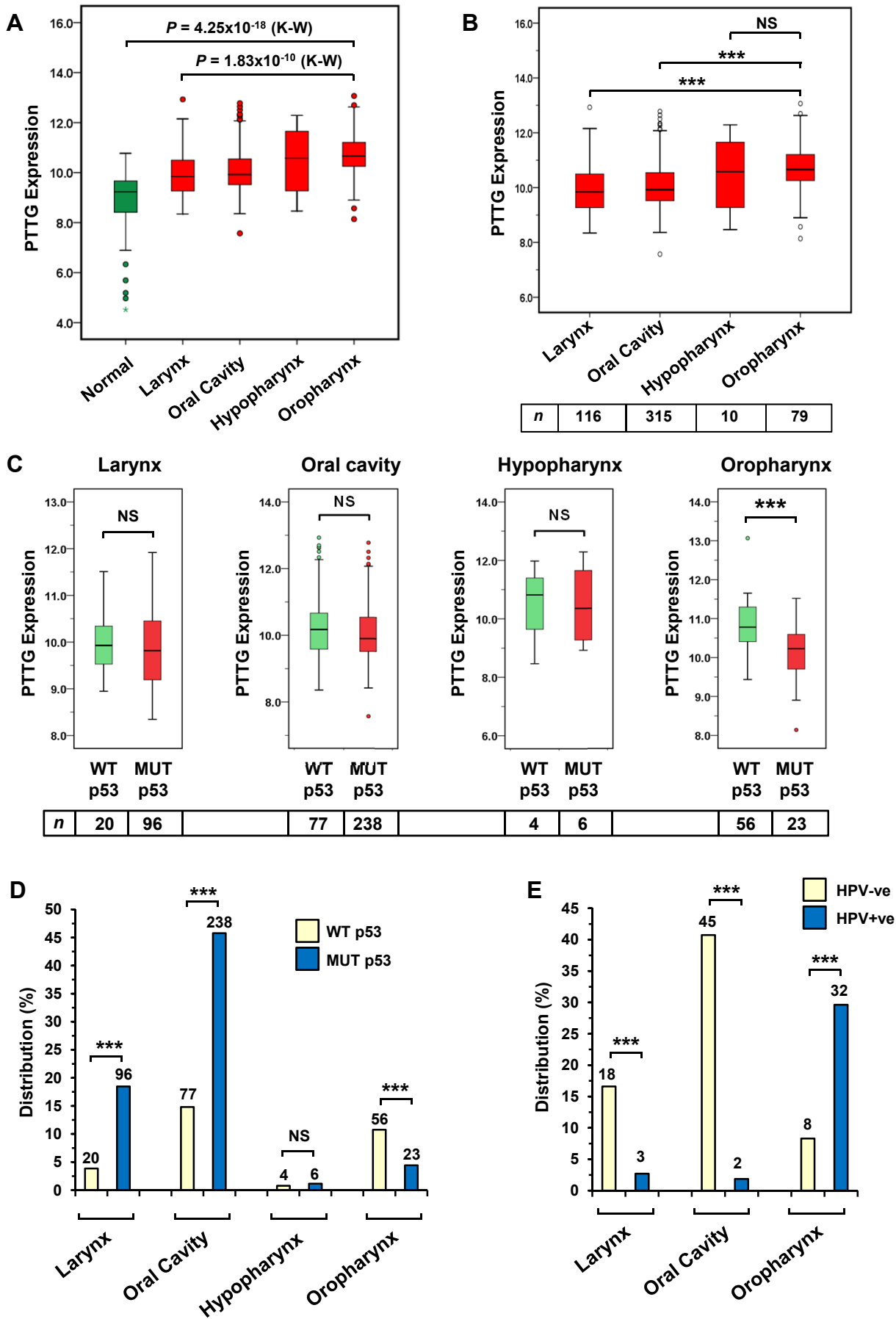
Supplementary Figure S2. PTTG expression at HNSCC anatomical subsites. **A,** Box whisker plot of PTTG expression ($\log_2$) in unmatched HNSCC at the larynx ($n = 116$), oral cavity ($n = 315$), hypopharynx ($n = 10$) and oropharynx subsites ($n = 79$) compared to normal specimens ($n = 43$) (***, $P = 4.39 \times 10^{-18}$; K-W, Kruskal-Wallis test). **B,** PTTG expression at the oropharynx versus other subsites (NS, not significant; ***, $P < 0.001$; Mann-Whitney test). **C,** Box whisker plot of PTTG expression ($\log_2$) in unmatched HNSCC with WT p53 or MUT p53 as indicated at different subsites. Number of HNSCC samples per subgroup are shown; NS, not significant; ***, $P < 0.001$. **D,** Distribution (%) of WT p53 or MUT p53 HNSCC at different HNSCC anatomical subsites (NS, not significant; ***, $P < 0.001$; Fisher's exact test). Number of HNSCC samples per subgroup are shown. **E,** Distribution (%) of HPV (-ve) or (+ve) HNSCC at different subsites (***, $P < 0.001$; Fisher's exact test). Number of HNSCC samples per subgroup are shown.

Supplementary Figure S3. Expression of PTTG in HNSCC. Representative images of total (left) and T60-phosphorylated (right) PTTG protein in HNSCC and normal tissue. Images taken at 20x (scale bars, 100 μm) and 80x (scale bars, 10 μm) magnification as indicated. Sections were counterstained for haematoxylin. Total and T60-phosphorylated PTTG protein were abundantly overexpressed in oropharyngeal tumours of all stages (1-4) as indicated.
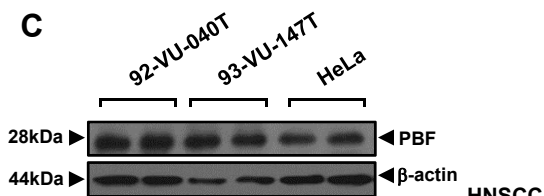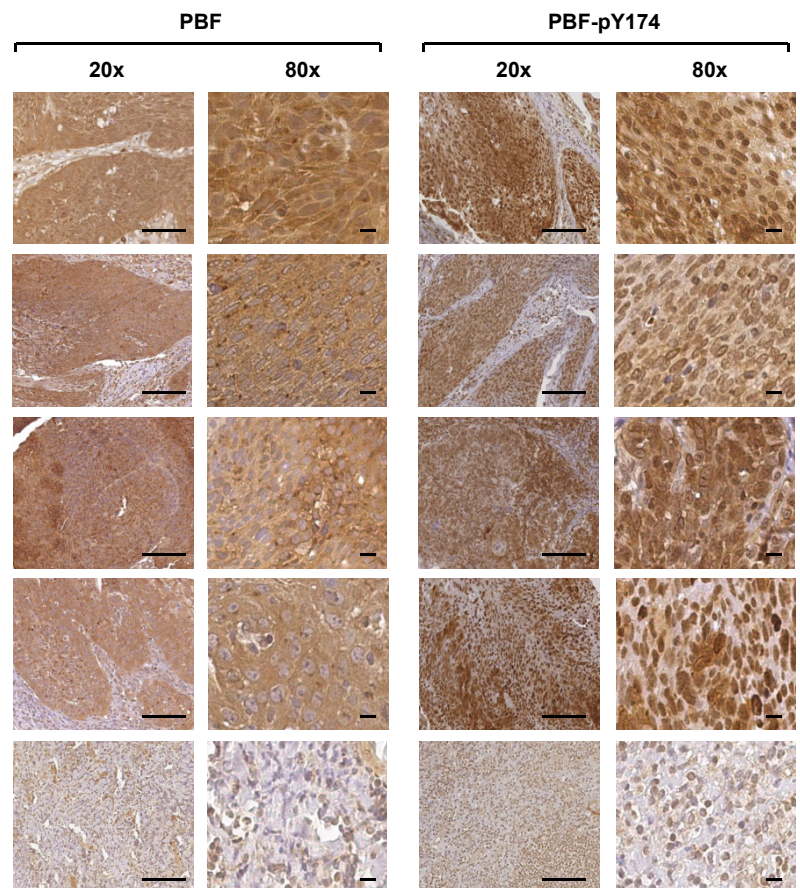
A — Box whisker plot of PBF Expression

n	43	116	315	10	79

Normal, Larynx, Oral Cavity, Hypopharynx, Oropharynx

B

Overall survival of HNSCC patients stratified on PBF expression

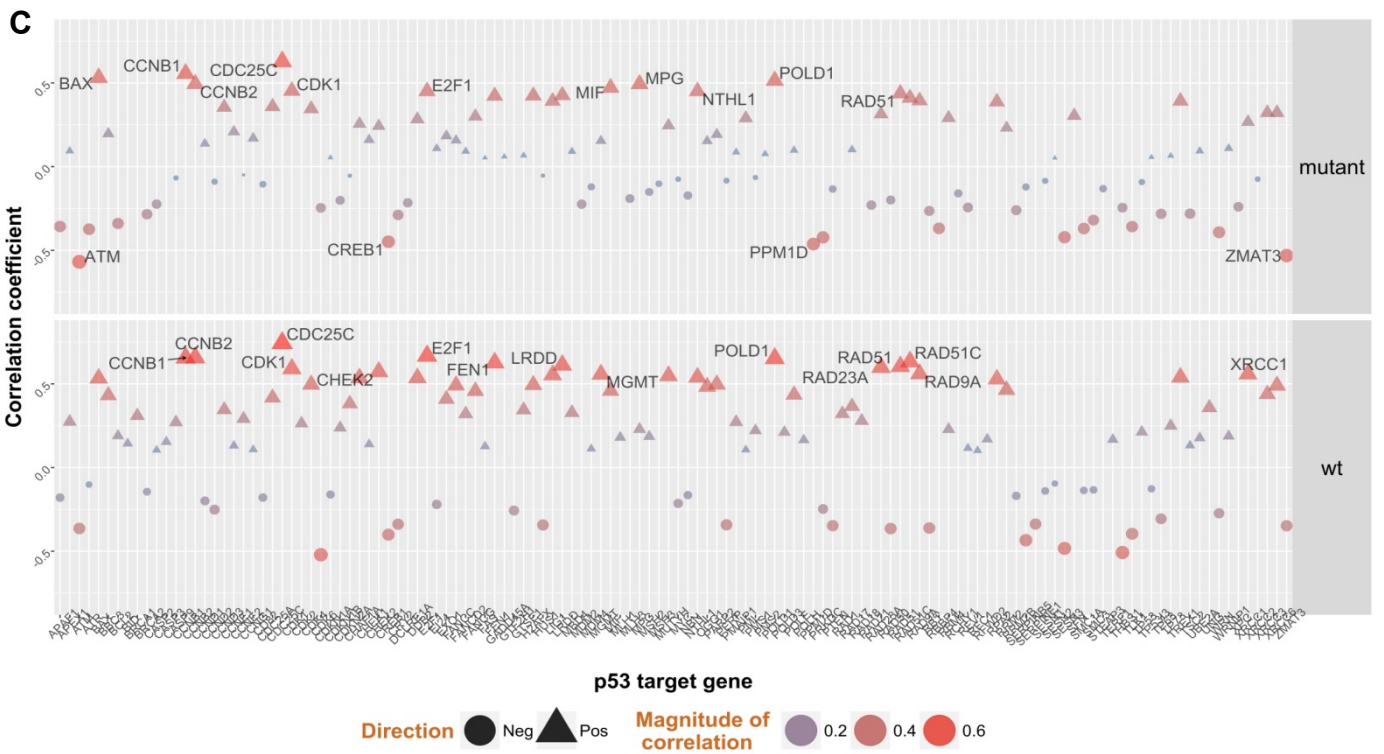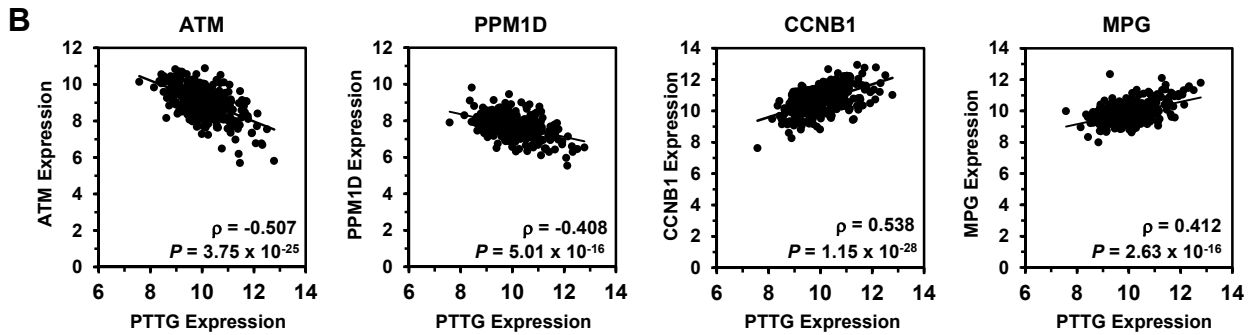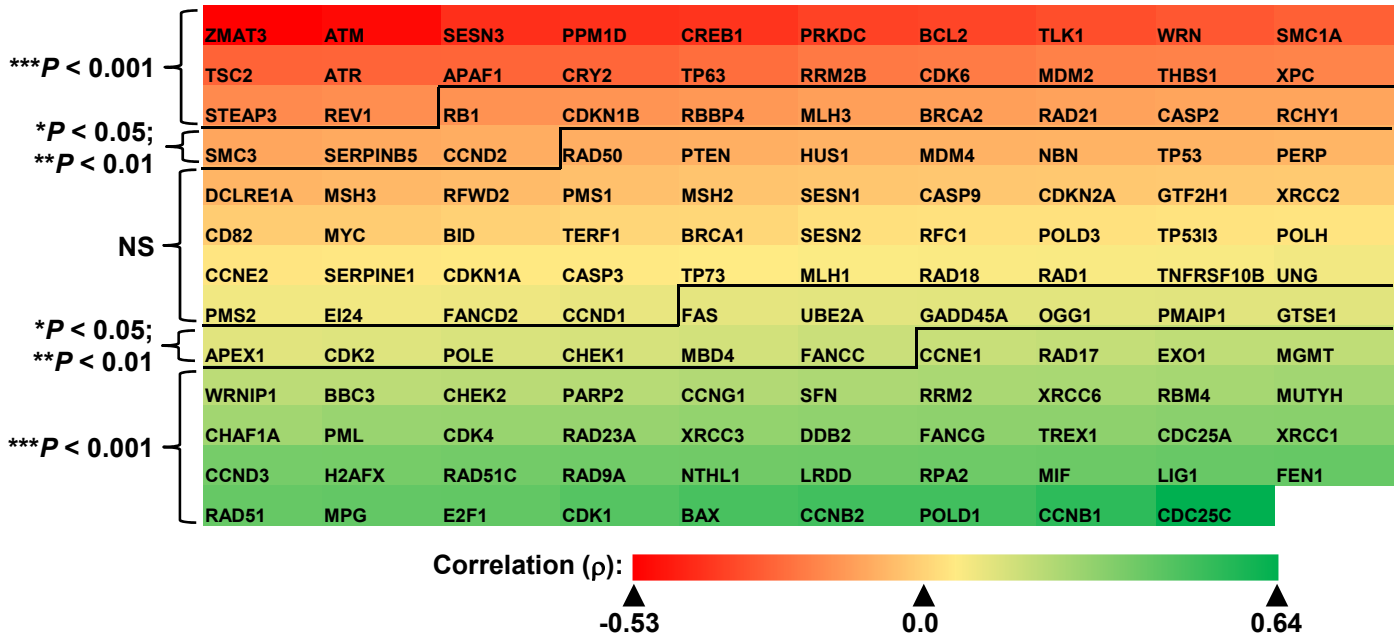| Patient stratification	N	P_L	P_B	P_T
HIGH PBF (Q4) vs LOW PBF (Q1-Q3)	129 / 388	0.025	0.013	0.016
HIGH PBF (Q4) vs LOW PBF (Q1)	129 / 129	NS	0.017	0.028
HIGH PBF (Q3Q4) vs LOW PBF (Q1Q2)	258 / 259	NS	0.030	NS

Supplementary Figure S4. Expression of PBF in HNSCC. **A,** Box whisker plot of PBF expression (log_2) in unmatched HNSCC at the larynx (n = 116), oral cavity (n = 315), hypopharynx (n = 10) and oropharynx subsites (n = 79) compared to normal specimens (n = 43) (NS, not significant; *, $P < 0.05$; Kruskal-Wallis test). **B,** Overall survival for HNSCC TCGA patients based on stratification criteria of PBF expression as indicated. Numbers of patients per subgroup are shown as well as P-values determined using the indicated test (L=Log Rank, B-Breslow, T=Tarone-Ware). Red box highlights a significant difference using the P_B test in overall survival for all PBF stratification groups. In the P_B test time points are weighted by the number of cases at risk at each time point which emphasizes shorter survival times. **C,** Western blot analysis of PBF expression in HNSCC cell lines used in study compared to HeLa cells. **D,** Representative images of total (left) and Y174-phosphorylated (right) PBF protein in HNSCC and normal tissue. Images taken at 20x (scale bars, 100 μm) and 80x (scale bars, 10 μm) magnification as indicated. Sections were counterstained for haematoxylin. Total and Y174-phosphorylated PBF protein were abundantly overexpressed in oropharyngeal tumours of all stages (1-4) as indicated.
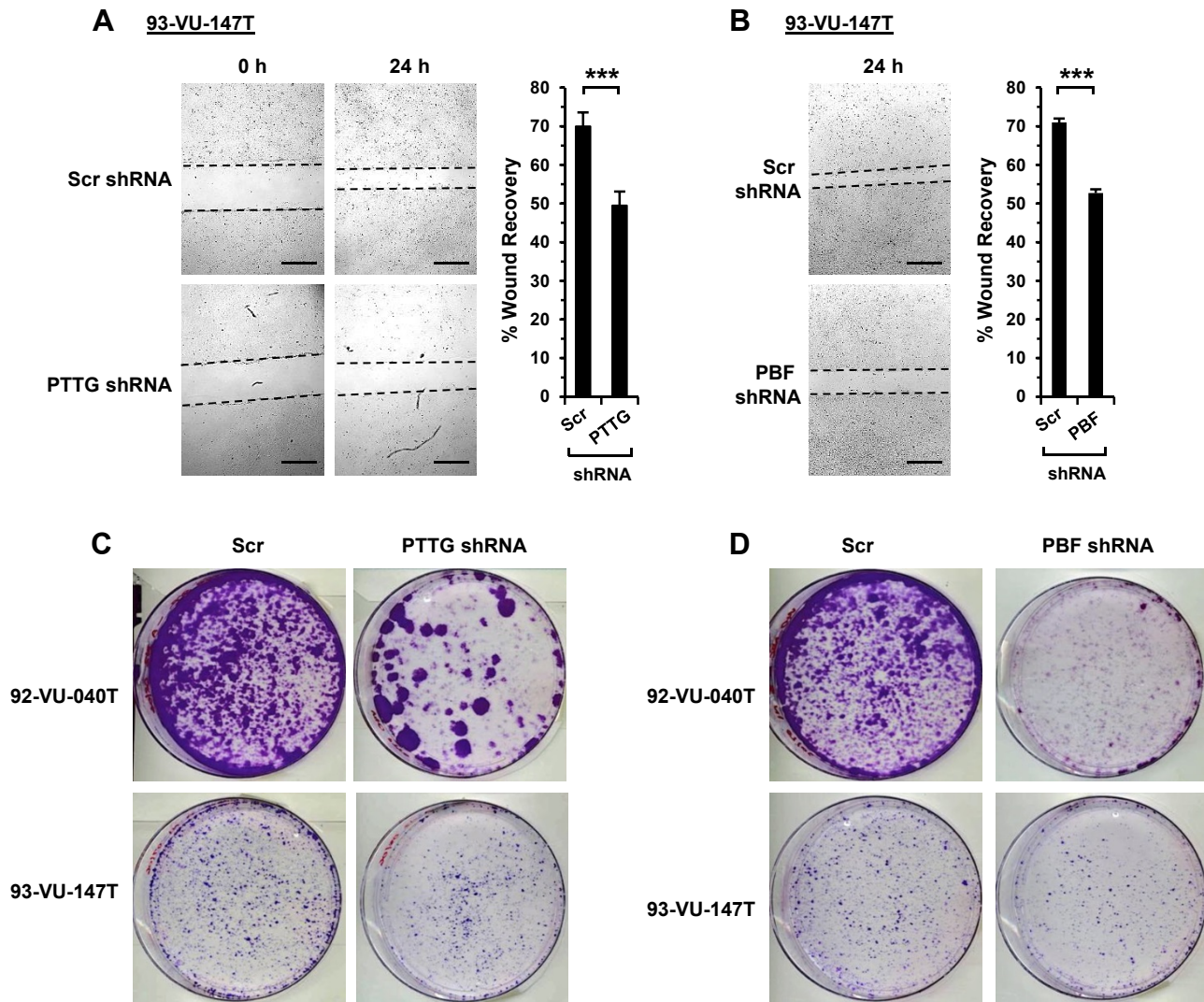
Supplementary Figure S5. Depletion of PTTG and PBF impairs wound healing and transforming abilities of HNSCC cells. **A,** Representative images of scratch wound assays in 93-VU-147T cells transduced with either PTTG or Scr shRNA. Images taken after 0 and 24 h. Scale bars, 500 μm. (right) % wound recovery determined at 24 h (mean ± s.e.m., n = 3 independent experiments; unpaired two-tailed t-test; ***, $P < 0.001$). **B,** Same as (**A**) but instead showing wound healing in PBF shRNA transduced 93-VU-147T cells. **C,** Representative colony formation assay images of 92-VU-040T and 93-VU-147T cells stably transduced with either PTTG or Scr shRNA from n = 3 experiments. **D,** Same as (**C**) but cells were stably transduced with PBF shRNA. In colony formation assays 1 x 10^4 HNSCC cells were seeded in 100 mm tissue culture dishes and incubated in a humidified atmosphere at 37°C and 5% CO_2. After 18 days incubation colonies were fixed with 100% methanol for 15 min at RT and stained with 0.05% crystal violet for 30 min. Excess crystal violet was removed by PBS washing and dishes allowed to air-dry prior to examination of colonies.

Supplementary Figure S6. Correlation of PTTG expression with p53-target genes in WT p53 HNSCC. **A,** Heatmap showing relative correlation values (ρ) for PTTG expression with a panel of 129 p53-target genes using TCGA data ($n = 157$ unmatched WT p53 HNSCC samples). Significant correlations with PTTG were observed for 82.2% (*, $P < 0.05$, $n = 106/129$ genes) and 57.4% (***, $P < 0.001$, $n = 74/129$ genes) of p53-target genes according to the level of significance. P and ρ values were calculated using the Spearman's correlation test. **B,** Representative scatterplots showing significant correlations for expression of *SESN3*, *CDK6*, *CDC25C*, and *E2F1* ($n = 157$ unmatched HNSCC samples; ***, $P < 0.001$; Spearman's correlation test). **C,** Box whisker plots of p53-target gene expression ($\log_2$) with $\Delta\rho > 0.45$ ($\rho_{WTp53}-\rho_{MUTp53}$) in unmatched HNSCC with either WT or MUT p53. Expression of *BCL2*, *CDKN2A*, and *PPM1D* was significantly lower in MUT p53 HNSCC ($n = 363$) compared to WT p53 HNSCC ($n = 157$) (***, $P < 0.001$; Mann-Whitney test). **D,** Same as (**C**) but showing p53-target gene expression ($\log_2$) with $\Delta\rho < -0.3$ ($\rho_{WTp53}-\rho_{MUTp53}$) in unmatched HNSCC. Expression of *SFN*, *EI24*, and *CCND1* was significantly increased in MUT p53 HNSCC ($n = 363$) compared to WT p53 HNSCC ($n = 157$) (**, $P < 0.01$; ***, $P < 0.001$; Mann-Whitney test).

Supplementary Figure S7. Correlation of PTTG expression with p53-target genes in MUT p53 HNSCC. **A,** Heatmap showing relative correlation values (ρ) for PTTG expression with a panel of 129 p53-target genes using TCGA data (n = 363 unmatched MUT p53 HNSCC samples). Significant correlations with PTTG were observed for 68.2% (*, $P < 0.05$; n = 88/129 genes) and 50.4% (***, $P < 0.001$; n = 65/129 genes) of p53-target genes according to the level of significance. P and ρ values were calculated using the Spearman's correlation test. **B,** Representative scatterplots showing significant correlations for expression of *ATM*, *PPM1D*, *CCNB1* and *MPG* (n = 363 unmatched HNSCC samples; ***, $P < 0.001$; Spearman's correlation test). **C,** Direct comparison of correlation values for PTTG expression with 129 p53-target genes in MUT p53 (upper) and WT p53 HNSCC (lower). p53 target genes are listed in alphabetical order.

A WT p53 HNSCC TCGA; *n* = 157; 23/129 genes (*P* < 0.05); MUT p53; *n* = 363; 49/129 genes (*P* < 0.05)
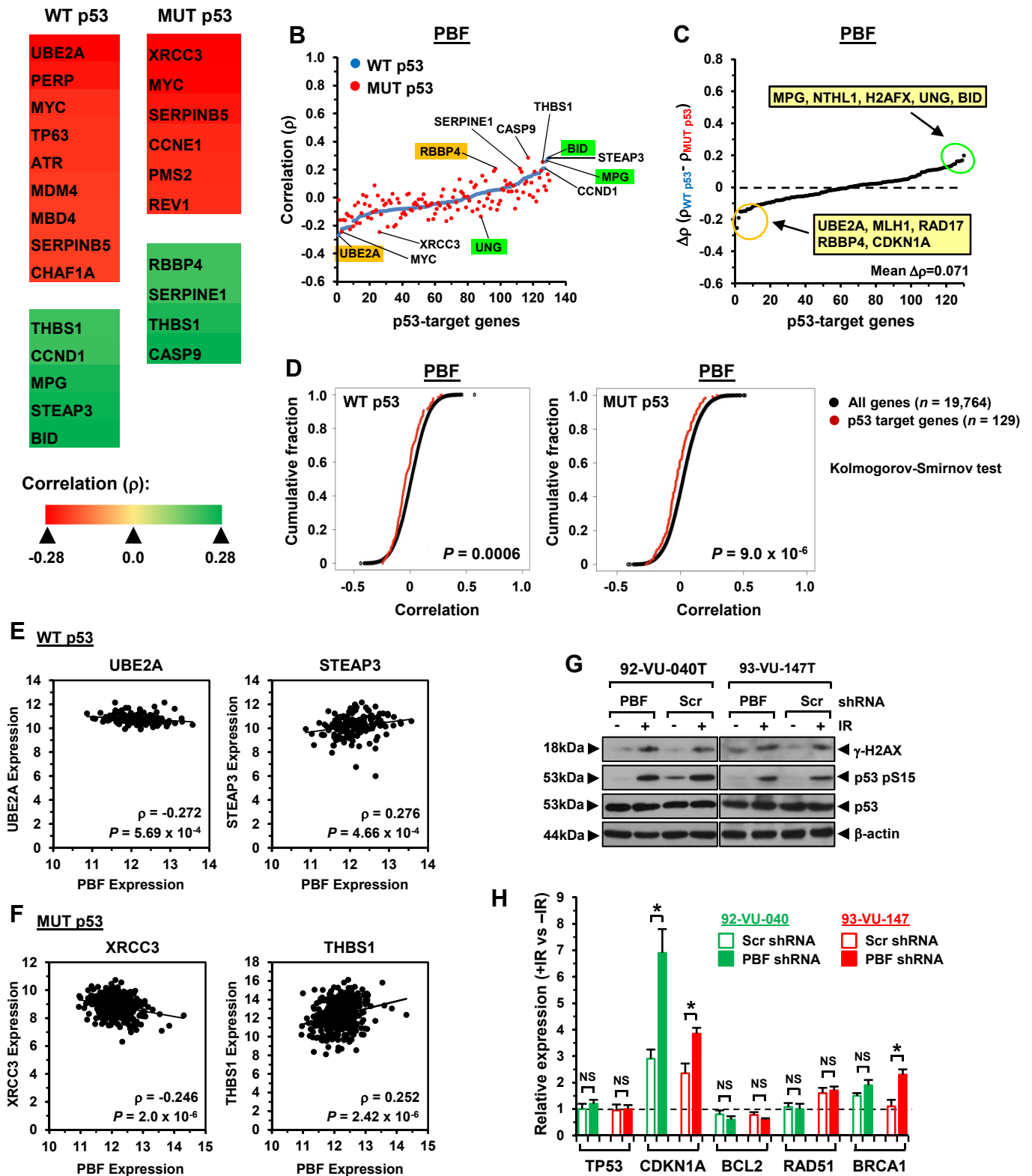
Supplementary Figure S8. Association of PBF with p53-target genes. C. **A,** Heatmap showing relative correlation values for PBF expression with p53-target genes in WT p53 (left, *n* = 157) and MUT p53 (right, *n* = 363) unmatched HNSCC. Genes shown have ρ values < -0.2 or > 0.2; *, *P* < 0.05. **B,** Correlation pattern of PBF expression with 129 p53-target genes in unmatched HNSCC with WT p53 (blue dots; *n* = 157) and MUT p53 (red dots; *n* = 363). **C,** Differences in ρ values for p53-target genes between WT and MUT p53 HNSCC. Genes were ordered according to increasing Δρ value (ρ$_{WTp53}$–ρ$_{MUTp53}$; range -0.25 to +0.28). **D,** Cumulative distribution plot comparing the correlations between PBF with all detectable genes in TCGA (*n* = 19,764) versus p53-target genes (*n* = 129) in WT (upper) and MUT p53 (lower) HNSCC. Significant difference between distributions determined by the Kolmogorov-Smirnov test. **E,** Representative scatterplots showing significant correlations for expression of *UBE2A* and *STEAP3* with PBF in WT p53 HNSCC (*n* = 157 unmatched HNSCC; **, *P* < 0.01; ***, *P* < 0.001; Spearman's correlation test). **F,** Same as (**E**) but showing scatterplots for expression of *XRCC3* and *THBS1* with PBF in MUT p53 HNSCC (*n* = 363 unmatched HNSCC; ***, *P* < 0.001; Spearman's correlation test). **G,** Western blot analysis of γ-H2AX, p53 S15 and p53 in PBF or Scr shRNA transduced 92-VU-040T and 93-VU-147T cells irradiated with 15-Gy dose. **H,** Relative fold-change in mRNA expression of indicated genes following irradiation of PBF or Scr shRNA stably transduced 92-VU-040T and 93-VU-147T cells compared with non-irradiated controls (mean ± s.e.m., *n* = 3 independent experiments; unpaired two-tailed *t*-test; ns-not significant; *, *P* < 0.05).
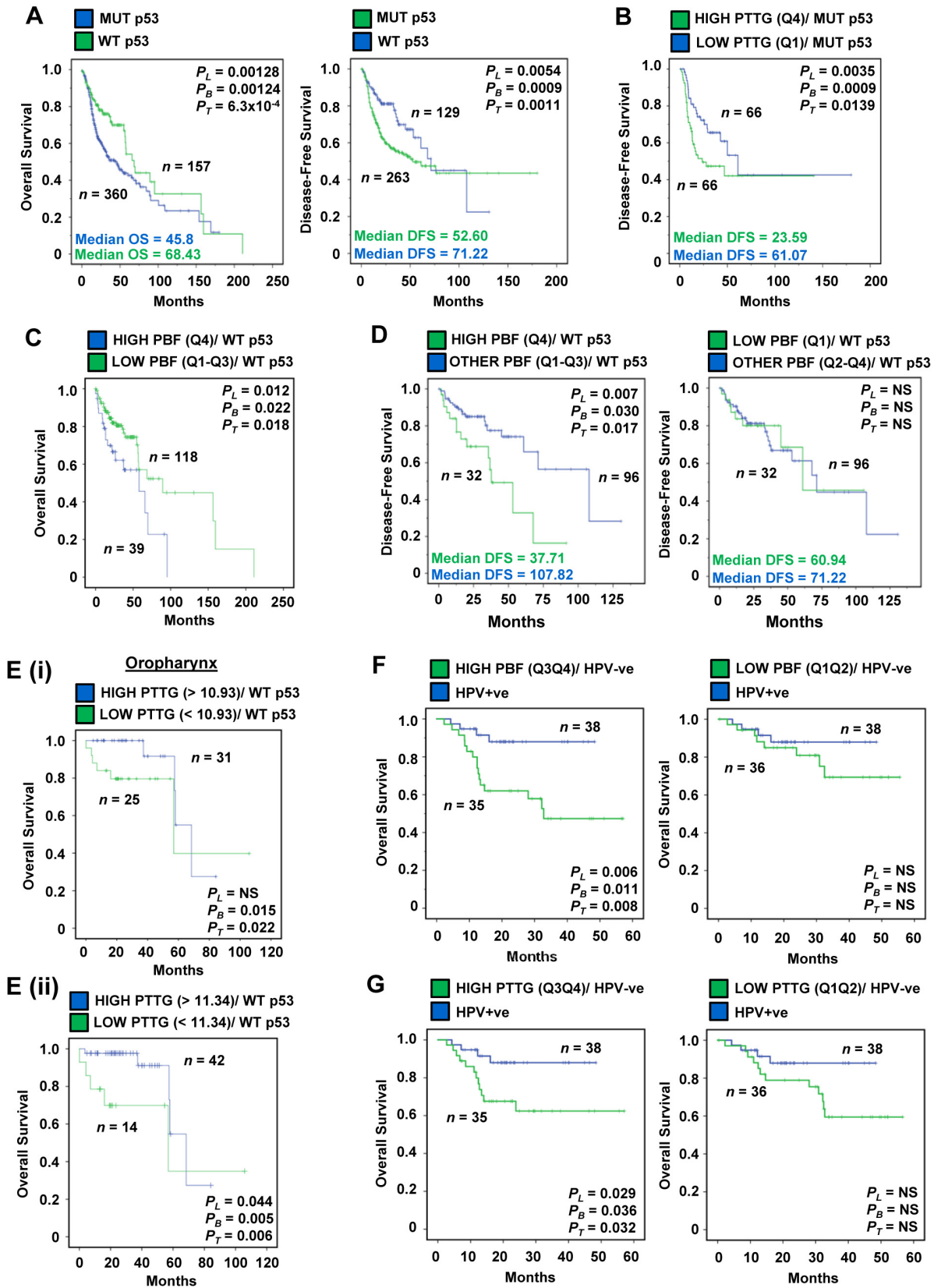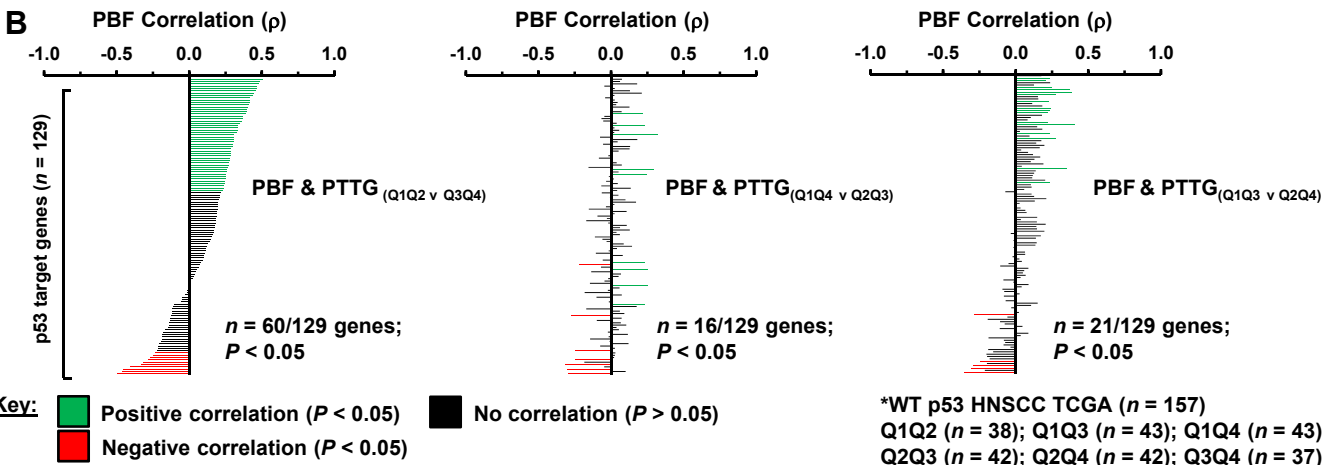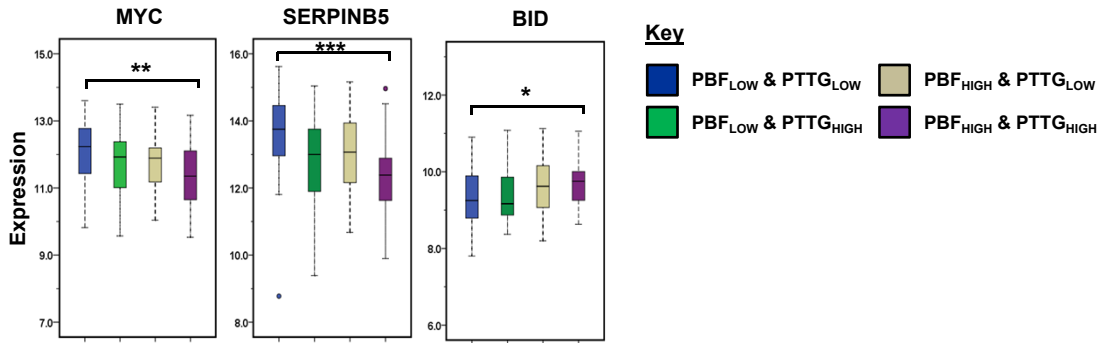
Supplementary Figure S9. PTTG and PBF expression associates with poorer survival. **A,** Overall (left) and disease-free (right) survival curves for MUT p53 HNSCC compared to WT p53 HNSCC. **B,** Disease-free survival for MUT p53 HNSCC with high PTTG expression (*n* = 66, Q4 quartile) compared to low PTTG expression (*n* = 66, Q1 quartile). **C,** Overall survival for WT p53 HNSCC with high (*n* = 39, Q4 quartile) versus low (*n* = 118, Q1-Q3 quartiles) PBF expression. **D,** Disease-free survival for WT p53 HNSCC with either high (Q4, left) or low (Q1, right) PBF expression compared to other WT p53 HNSCC cases. **E(i),** Overall survival for WT p53 oropharyngeal HNSCC with high (*n* = 25) versus low PTTG expression (*n* = 31). Cut off value for stratification based on Q4 quartile value (> 10.93) of PTTG expression for entire WT p53 HNSCC cohort (*n* = 157). **E(ii),** Same as E(i) but using higher cut off value for stratification (Q4 > 11.34) based on PTTG expression for just the oropharyngeal WT p53 HNSCC cohort (*n* = 56) to adjust for any potential bias in observed differences in PTTG expression at different tumour subsites. **F,** Overall survival for HPV-ve HNSCC with high (left, *n* = 35, Q3Q4 quartile) versus low PBF expression (right, *n* = 36, Q1Q2 quartile) compared to HPV+ve HNSCC (*n* = 38). **G,** Overall survival for HPV-ve HNSCC with high (left, *n* = 35, Q3Q4 quartile) versus low PTTG expression (right, *n* = 36, Q1Q2 quartile) compared to HPV+ve HNSCC (*n* = 38). All *P*-values were determined using the indicated test (L=Log Rank, B=Breslow, T=Tarone-Ware). Number of HNSCC patients per subgroup are shown as well as median OS and DFS values (months).
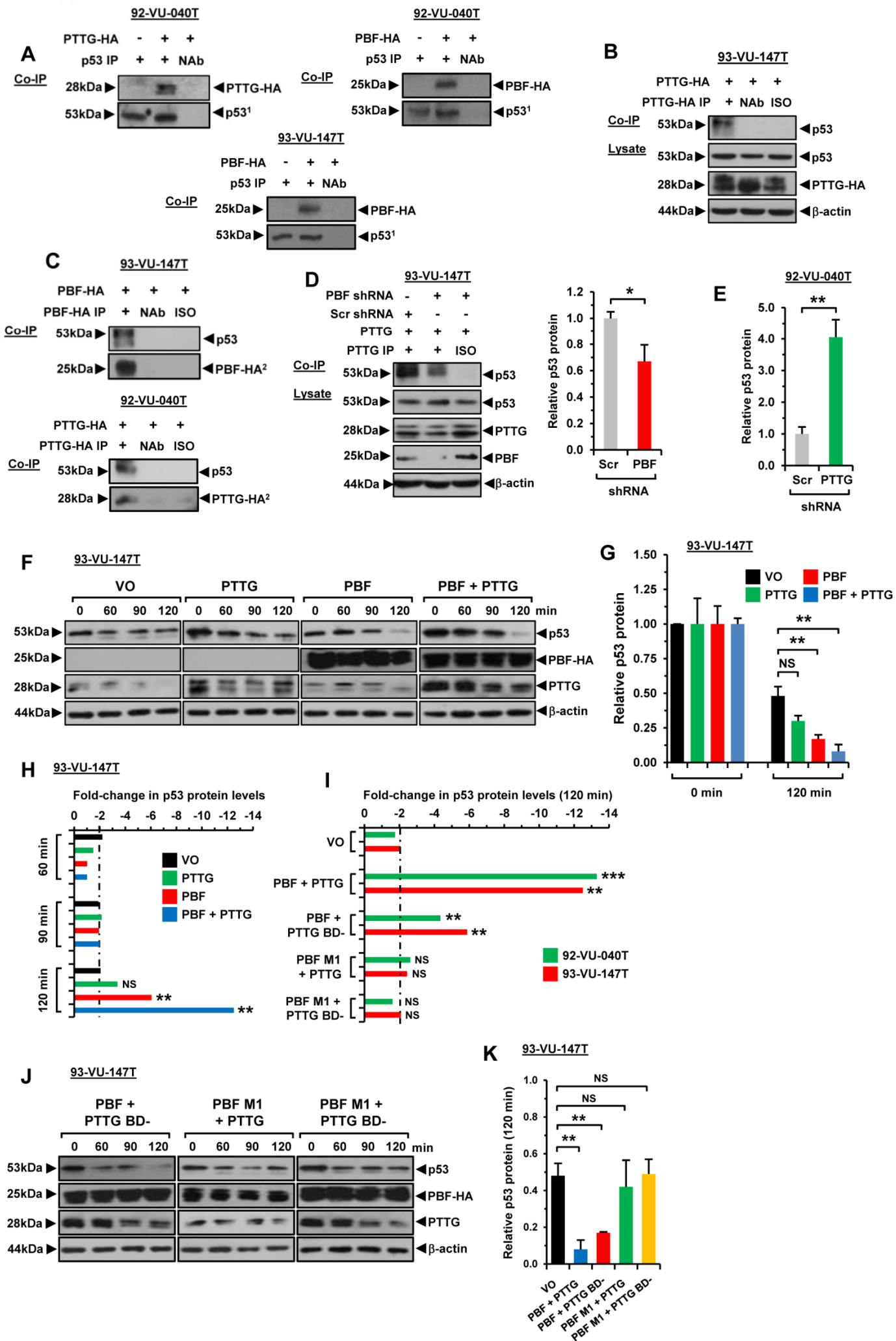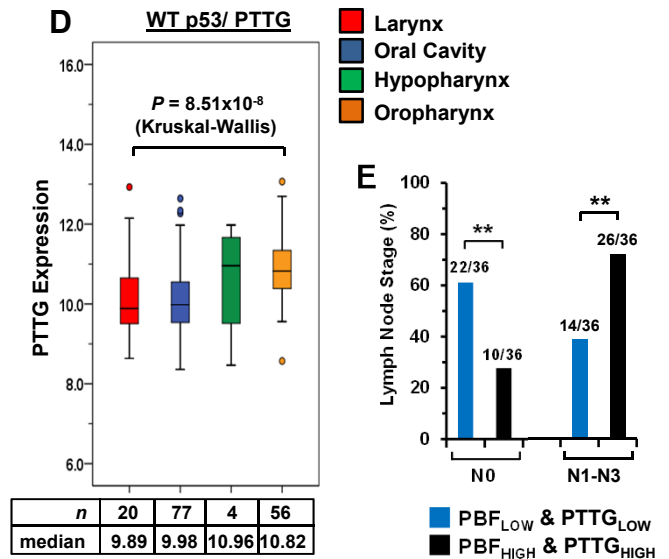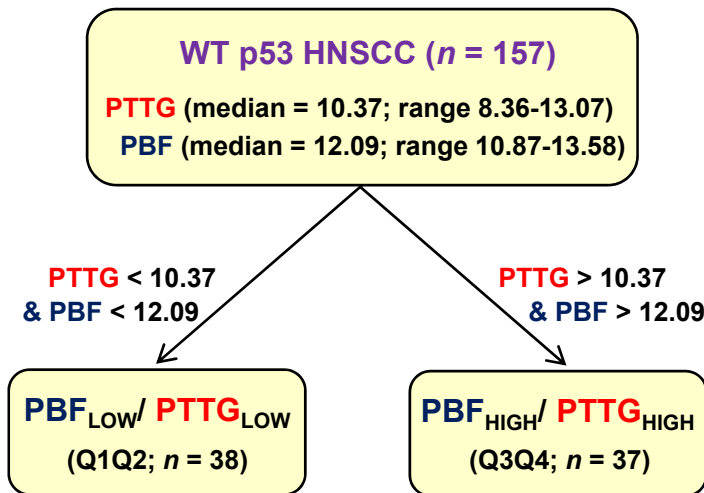
Supplementary Figure S10. PTTG and PBF influence p53 stability. **A,** Western blot analysis confirming successful immunoprecipitation of p53 in HNSCC cells. [1]Blot probed with an anti-p53 rabbit polyclonal antibody (Santa Cruz Biotechnology). **B,** Reciprocal co-IP assay in 93-VU-147T cells showing specific interaction between PTTG and p53. Cell lysates were immunoprecipitated with an anti-HA antibody. **C,** Western blot analysis confirming successful immunoprecipitation of PBF-HA and PTTG-HA in HNSCC cells. [2]Blot probed with an anti-HA rabbit polyclonal antibody (Santa Cruz Biotechnology). **D,** Co-IP assay in PBF shRNA stably transduced 93-VU-147T cells showing reduced interaction between PTTG and p53. (right) Mean p53 protein levels relative to β-actin (mean ± s.e.m., n = 3 independent experiments; unpaired two-tailed t-test; *, $P < 0.05$). **E,** Quantification of mean p53 protein levels from co-IP assays in PTTG shRNA transduced 92-VU-040T cells showing greater interaction between PBF and p53. (mean ± s.e.m., n = 3 independent experiments; unpaired two-tailed t-test; **, $P < 0.01$). **F,** Western Blot analysis of p53 stability in 93-VU-147T cells transfected with VO, PBF-HA, PTTG or PBF-HA+PTTG and then lysed at indicated times post-treatment with 100 μM anisomycin. (right) Quantification of mean p53 protein levels relative to β-actin from 3 independent experiments at indicated time points (mean ± s.e.m., n = 3 independent experiments; unpaired two-tailed t-test; NS, not significant; **, $P < 0.01$). **H,** Fold-changes in relative p53 protein levels normalised to β-actin at indicated time points post-anisomycin treatment in 93-VU-147T cells transfected with VO, PTTG, PBF or PBF+PTTG . **I,** Fold-changes in relative p53 protein levels normalised to β-actin at 120 min post-anisomycin treatment in 92-VU-040T and 93-VU-147T cells transfected with VO, PBF+PTTG, PBF+PTTG BD-, PBF M1+PTTG or PBF M1+PTTG BD- (mean., n = 3 independent experiments, **, $P < 0.01$; ***, $P < 0.001$). **J,** Western Blot analysis of p53 stability in 93-VU-147T cells transfected with PBF+PTTG BD-, PBF M1+PTTG or PBF M1+PTTG BD- and then lysed at indicated times post-treatment with 100 μM anisomycin. **K,** Mean p53 protein levels normalised to β-actin from half-life study described in (J). Data presented as mean ± SE from 3 independent experiments; **, $P < 0.001$..

A WT p53 HNSCC TCGA (*n* = 157)

Key
- PBF_LOW & PTTG_LOW
- PBF_LOW & PTTG_HIGH
- PBF_HIGH & PTTG_LOW
- PBF_HIGH & PTTG_HIGH

B

PBF & PTTG(Q1Q2 v Q3Q4)
n = 60/129 genes; *P* < 0.05

PBF & PTTG(Q1Q4 v Q2Q3)
n = 16/129 genes; *P* < 0.05

PBF & PTTG(Q1Q3 v Q2Q4)
n = 21/129 genes; *P* < 0.05

Key:
- Positive correlation (*P* < 0.05)
- Negative correlation (*P* < 0.05)
- No correlation (*P* > 0.05)

*WT p53 HNSCC TCGA (*n* = 157)
Q1Q2 (*n* = 38); Q1Q3 (*n* = 43); Q1Q4 (*n* = 43)
Q2Q3 (*n* = 42); Q2Q4 (*n* = 42); Q3Q4 (*n* = 37)

C Stratification of PBF/PTTG subgroups in lymph node staging analysis (WT p53 HNSCC)

WT p53 HNSCC (*n* = 157)

PTTG (median = 10.37; range 8.36-13.07)
PBF (median = 12.09; range 10.87-13.58)

PTTG < 10.37 & PBF < 12.09

PTTG > 10.37 & PBF > 12.09

PBF_LOW/ PTTG_LOW (Q1Q2; *n* = 38)

PBF_HIGH/ PTTG_HIGH (Q3Q4; *n* = 37)

D WT p53/ PTTG

- Larynx
- Oral Cavity
- Hypopharynx
- Oropharynx

P = 8.51x10⁻⁸ (Kruskal-Wallis)

n	20	77	4	56
median	9.89	9.98	10.96	10.82

E

- PBF_LOW & PTTG_LOW
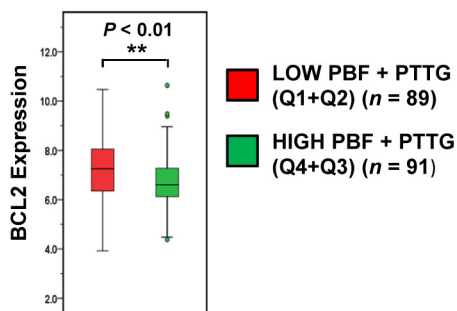- PBF_HIGH & PTTG_HIGH

N0: 22/36, 10/36
N1-N3: 14/36, 26/36

Supplementary Figure S11. Correlation of p53-target genes with PBF in WT p53 HNSCC with high PBF/PTTG expression. **A,** Box-whisker plots for indicated genes (i.e. *MYC*, *SERPINB5* and *BID*) in WT p53 HNSCC with high PBF/high PTTG tumoural expression (*n* = 37; Q3+Q4) compared to other HNSCC subgroups [(i.e. low PBF/low PTTG (*n* = 38; Q1+Q2), low PBF/high PTTG (*n* = 41) and high PBF/low PTTG (*n* = 41)] (***, *P*<0.001; **, *P*<0.01; ***, *P*<0.001; Kruskal-Wallis test). **B,** Correlation of PBF expression with 129 p53-target genes in unmatched WT p53 HNSCC with high PBF/PTTG (*n* = 38; Q3+Q4) and low PBF/PTTG expression (*n* = 37; Q1+Q2; 75 HNSCC samples in total). *P* and ρ values were calculated using Spearman's correlation tests. Correlations were further determined in HNSCC with different PBF/PTTG expression subgroups, including (middle) PBF/PTTG (Q1+Q4, *n* = 43) and PBF/PTTG (Q2+Q3, *n* = 42) (85 HNSCC samples in total), as well as (right) PBF/PTTG (Q1+Q3, *n* = 43) and PBF/PTTG (Q2+Q4, *n* = 42) (85 HNSCC samples in total). **C,** Overview of patient stratification based on PBF and PTTG expression in WT p53 HNSCC (*n* = 157) for lymph node analysis (Figure 6H). Median cut off values for PTTG and PBF in different expression subgroups are shown as well as patient numbers. **D,** Box whisker plot of PTTG expression (log₂) at the indicated anatomical subsite in WT p53 HNSCC samples. (***, *P* = 8.51x10⁻⁸; Kruskal-Wallis test). Median values and number of samples are shown. **E,** Association of PBF/PTTG expression subgroups with lymph node staging in WT p53 HNSCC; **, *P* < 0.01; Fisher's exact test. Cut-off values were adjusted for stratification according to median values shown in (D) for each different tumour subsite to correct for any potential bias.
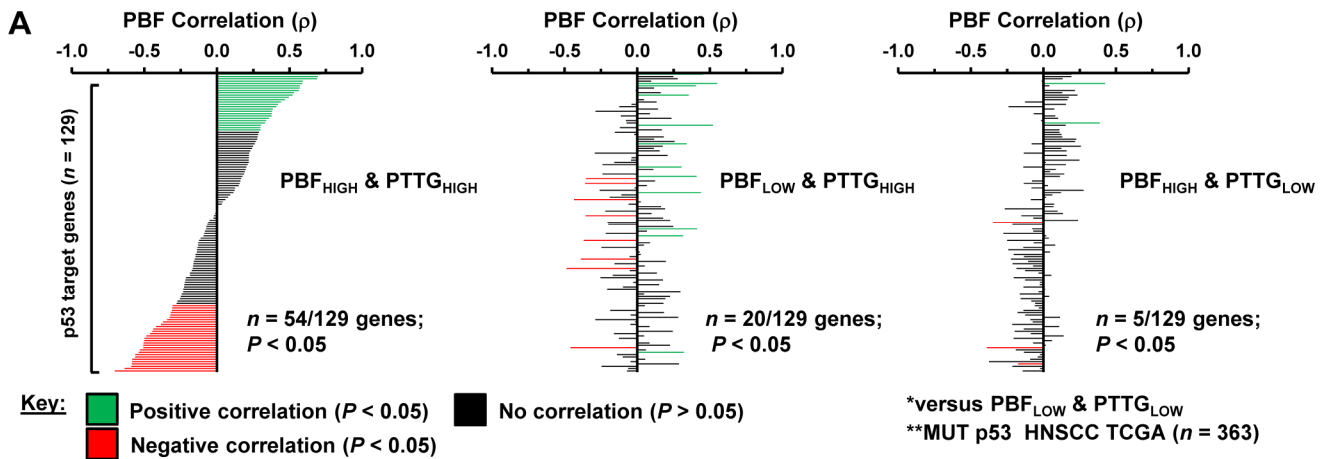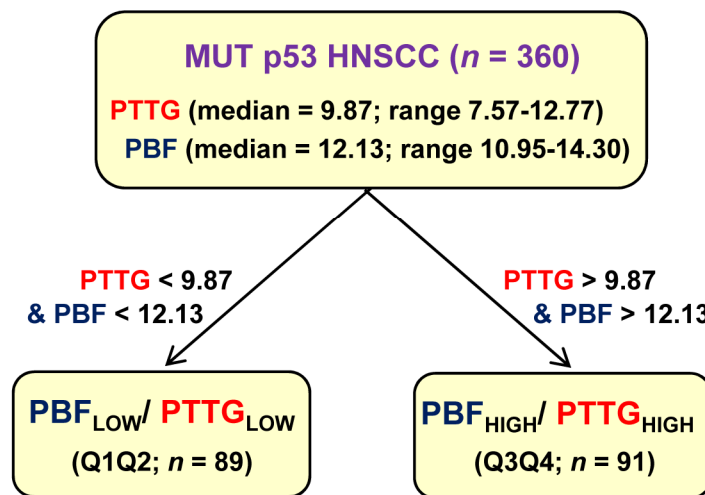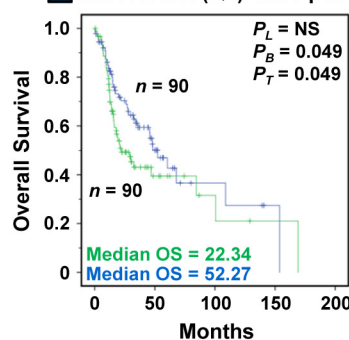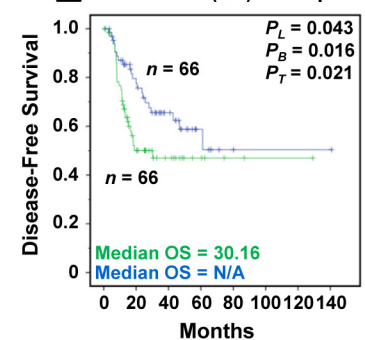
Supplementary Figure S12. Correlation of p53-target genes with PBF in MUT p53 HNSCC with high PBF/PTTG expression. **A,** Correlation of PBF expression with 129 p53-target genes in unmatched MUT p53 HNSCC with high PBF/high PTTG ($n = 24$, Q4Q4) and low PBF/low PTTG expression ($n = 20$, Q1Q1; 44 HNSCC samples in total). P and ρ values were calculated using Spearman's correlation tests. Correlations were further determined in HNSCC with (middle) low PBF/high PTTG ($n = 19$, Q1Q4) and low PBF/low PTTG expression (39 HNSCC samples in total), as well as in HNSCC with (right) high PBF/low PTTG ($n = 23$, Q4Q1) and low PBF/low PTTG (43 HNSCC samples in total). **B,** Overview of patient stratification based on PBF and PTTG expression in MUT p53 HNSCC ($n = 360$) for survival analysis (Figure 6I). Median cut off values for PTTG and PBF in different expression subgroups are shown as well as patient numbers. **C,** BCL2 mRNA expression in MUT p53 HNSCC with high versus low PBF/PTTG expression; **$P < 0.01$. **D,** Overall survival for MUT p53 HNSCC with low BCL2 expression ($n = 90$, Q1 quartile) compared to high ($n = 90$, Q4 quartile). P-values were determined using the indicated test (L=Log Rank, B=Breslow, T=Tarone-Ware). **E,** Disease-free survival for MUT p53 HNSCC with low BCL2 expression (Q1 quartile; MUT p53, $n = 66$) compared to high BCL2 expression (Q4 quartile; MUT p53, $n = 66$). All P-values were determined using the indicated test (L=Log Rank, B=Breslow, T=Tarone-Ware). Number of HNSCC patients per subgroup are shown as well as median OS and DFS values (months).

A

TP53

UniProt: P53_HUMAN
Transcript: ENST00000269305
Somatic Mutation Frequency: 69.1%

253 Missense   182 Truncating
10 Inframe   1 Other

B

C

	Number of patients
Missense	156
Nonsense	48
Splice	25
FS deletion	35
FS insertion	15
IF deletion	6
IF insertion	2

TP53 alterations per tumour = 1

D

TP53 alterations per tumour
■ 1
■ 2
■ 3

E

TP53 alterations per tumour = 1
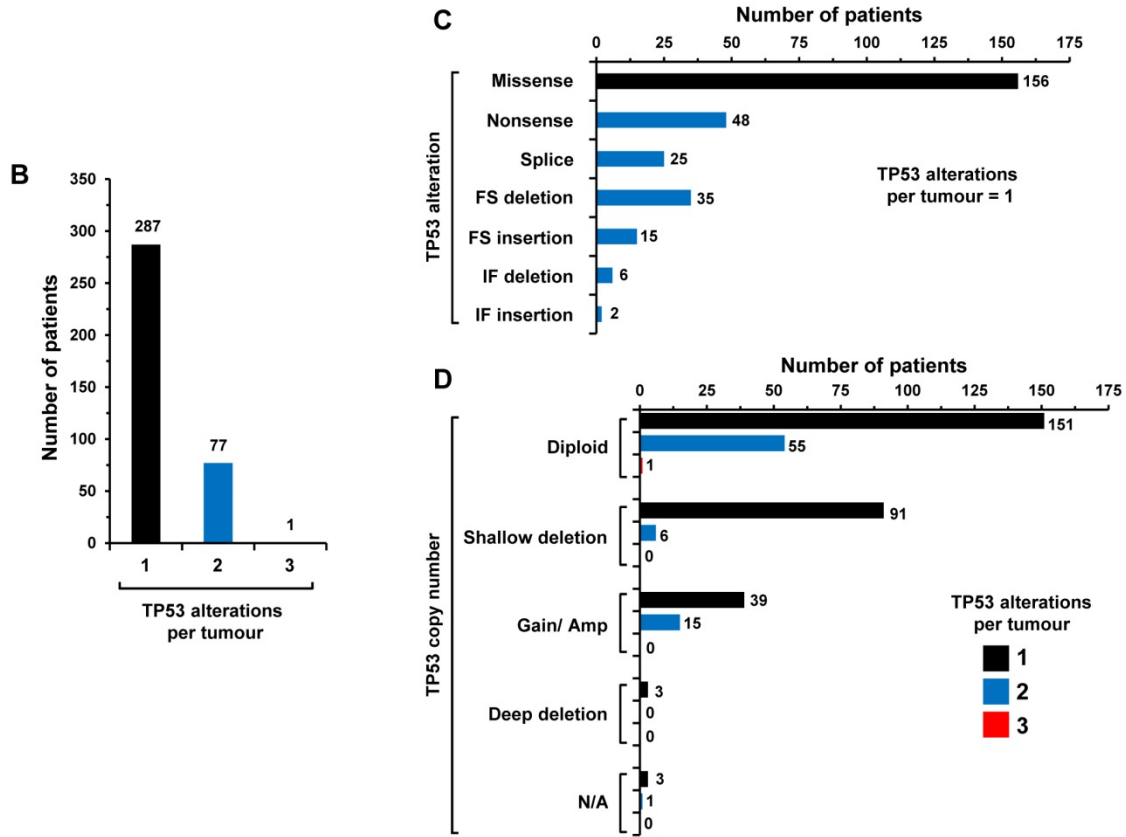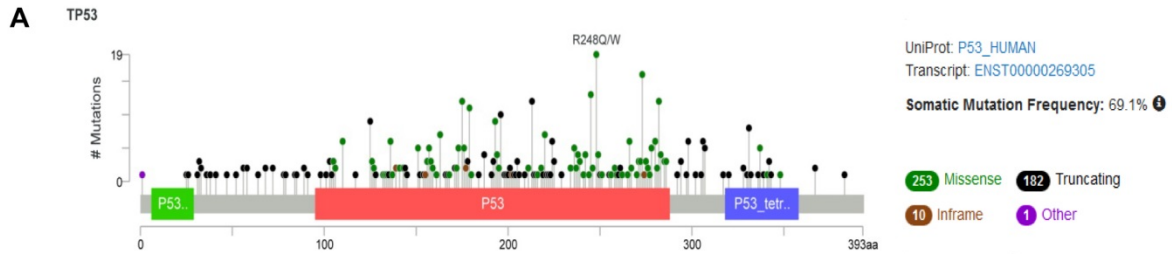
	Diploid	Shallow deletion	Gain/ Amp	Deep deletion	N/A
Missense	77	57	16	3	3
Nonsense	22	20	6	0	0
Splice	18	2	5	0	0
FS deletion	22	8	5	0	0
FS insertion	7	3	5	0	0
IF deletion	4	0	2	0	0
IF insertion	1	1	0	0	0

Supplementary Figure S13. Characterisation of TP53 mutations and copy number in HNSCC TCGA. **A,** Graphical representation of 446 mutations in HNSCC TCGA: includes 2 duplicate mutations in patients with multiple samples. Mutation diagram circles are coloured with respect to the corresponding mutation types. In case of different mutation types at a single position, colour of the circle is determined with respect to the most frequent mutation type (cBioPortal). Mutation types are: missense (green); truncating mutations (black) – i.e. nonsense, frameshift deletion, frameshift insertion, splice site; inframe Mutations (brown) – i.e. inframe deletion, inframe insertion. **B,** Number of patients in HNSCC TCGA with the indicated number of TP53 mutations per tumour sample. **C,** Number of patients in HNSCC TCGA with a single TP53 mutation per tumour ($n = 287$) and the indicated TP53 alteration (i.e. missense, nonsense, frame-shift and inframe). **D,** Number of patients in HNSCC TCGA with indicated putative TP53 copy number (i.e. diploid. Shallow deletion, deep deletion, gain, amp) and TP53 alterations per tumour. **E,** Table showing number of patients in HNSCC TCGA with a single TP53 mutation per tumour and the indicated TP53 alteration and putative copy number.
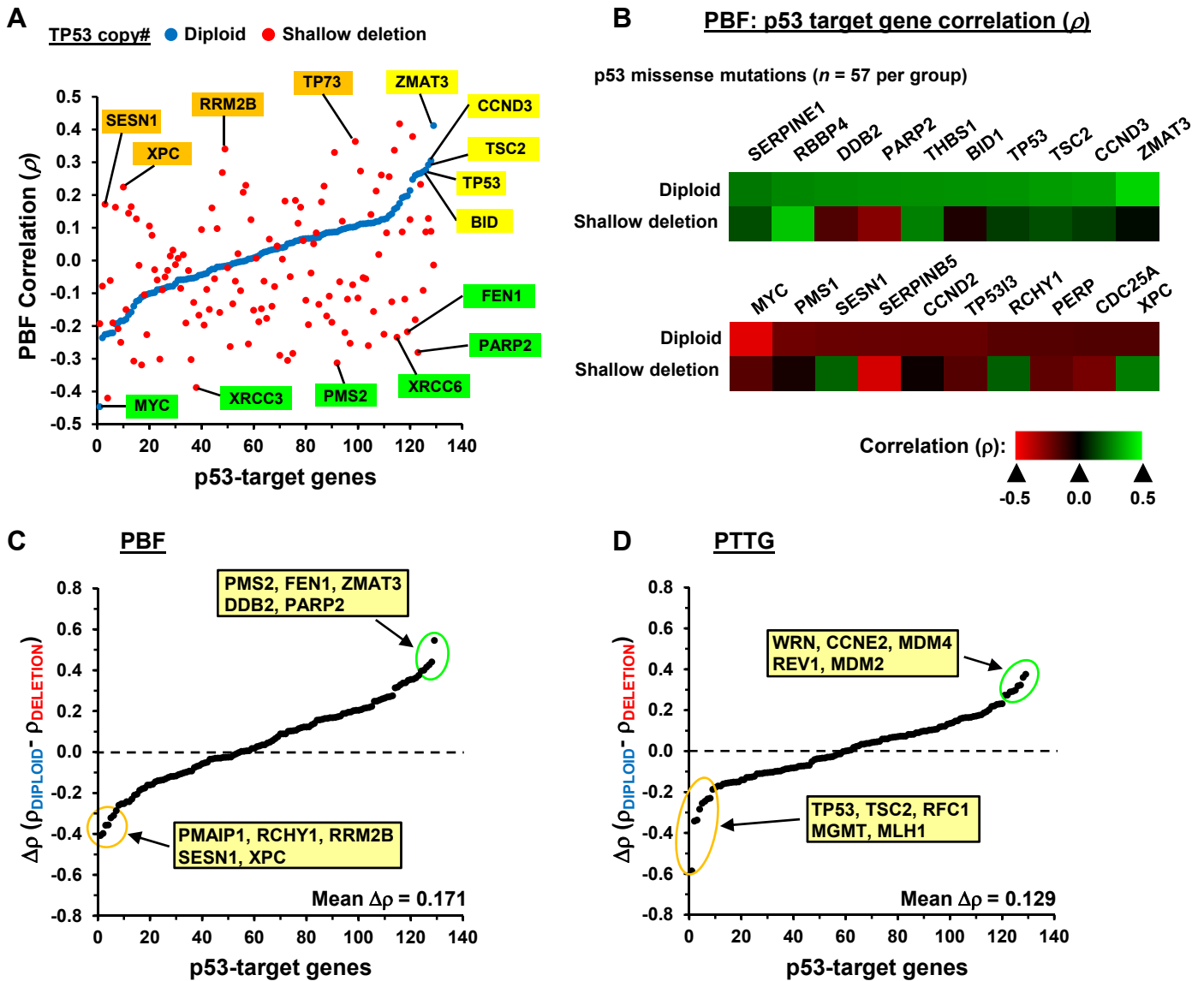
Supplementary Figure S14. Influence of TP53 genomic copy number on correlation of PBF and PTTG with p53-target genes. A, Correlation pattern of PBF with 129 p53-target genes in unmatched HNSCC with MUT p53 (single missense mutation per tumour) and either diploid (blue dots) or shallow deletion for TP53 (red dots) (*n* = 57 per group). **B,** Heatmap showing relative correlation values (ρ) for PBF with top ten most correlated p53-target genes (i.e. upper, positively correlated genes; lower, negatively correlated genes) in HNSCC TCGA with diploid versus shallow deletion for TP53 copy number. **C,** Differences in ρ values for PBF and p53-target genes in MUT p53 HNSCC with a single missense mutation and different TP53 copy number (i.e. diploid versus shallow deletion; *n* = 57 per group). Genes ordered according to increasing $\Delta\rho$ value ($\rho_{DIPLOID}$-$\rho_{DELETION}$; range -0.41 to +0.54). **D,** Differences in ρ values for PTTG and p53-target genes in MUT p53 HNSCC with a single missense mutation and different TP53 copy number (i.e. diploid versus shallow deletion; *n* = 57 per group). Genes ordered according to increasing $\Delta\rho$ value ($\rho_{DIPLOID}$-$\rho_{DELETION}$; range -0.59 to +0.38). The genomic copy number loss of wild-type TP53 disrupts the transcriptional relationship between PBF and PTTG with p53-target genes in tumour cells.